# Modeling of Condensation in the Presence of Noncondensables in GFSSP

Michael R. Baldwin[1] and S. Mostafa Ghiaasiaan[2]
*Georgia Institute of Technology, Atlanta, GA, 30332*

*and*

Alok K. Majumdar[3] and Andre C. LeClair[4]
*National Aeronautics and Space Administration, Marshall Space Flight Center, Huntsville, AL, 35812*

**The Generalized Fluid System Simulation Program (GFSSP) computer code is enhanced with the capability to model condensation in the presence of noncondensable gases. Condensation in the presence of noncondensables is modeled using the Couette flow film (stagnant film) model. Experimental data on the condensation of water vapor in downward flow of air-water vapor and helium-water vapor mixtures in vertical tubes are compared with the predictions of GFSSP. The comparisons show that GFSSP can predict the experimental data well.**

## Nomenclature

| | | |
|---|---|---|
| $A$ | = | area |
| $a_I^{"}$ | = | interfacial area concentration |
| $C_{Pv}$ | = | specific heat of the free stream mixture |
| $C_{PF}$ | = | specific heat of the liquid film |
| $D$ | = | pipe diameter |
| $h_{fg}$ | = | enthalpy of vaporization |
| $h_{\mathrm{FI}}$ | = | liquid film-to-interface heat transfer coefficient without effects of mass transfer |
| $\dot{h}_{\mathrm{FI}}$ | = | liquid film-to-interface heat transfer coefficient with effects of mass transfer |
| $h_{\mathrm{GI}}$ | = | mixture-to-interface heat transfer coefficient without effects of mass transfer |
| $\dot{h}_{\mathrm{GI}}$ | = | mixture-to-interface heat transfer coefficient with effects of mass transfer |
| $J$ | = | mechanical equivalent of heat (778 ft-$lb_f$/Btu) |
| $K_f$ | = | flow resistance coefficient |
| $K_{GI}$ | = | mass transfer coefficient |
| $M_n$ | = | molar mass of the noncondensable |
| $M_v$ | = | molar mass of the condensable |
| $m$ | = | mass |
| $\dot{m}$ | = | mass flow rate |
| $m^{"}$ | = | rate of condensation flux |
| $\dot{m}_G$ | = | free stream mixture mass flow rate |
| $\dot{m}_L$ | = | liquid film mass flow rate |
| $m_{v,G}$ | = | vapor mass fraction of the free stream mixture |
| $m_{v,s}$ | = | interfacial vapor mass fraction |
| $P$ | = | total pressure |
| $\bar{T}_F$ | = | film temperature |

---

[1] Graduate Student Assistant, Department of Mechanical Engineering, Georgia Institute of Technology.
[2] Professor, Department of Mechanical Engineering, Georgia Institute of Technology.

[3] Thermal Analysis Engineer, NASA Marshall Space Flight Center, ER43.
[4] Thermal Analysis Engineer, NASA Marshall Space Flight Center, ER43.

| | | |
|---|---|---|
| $\bar{T}_G$ | = | free stream mixture temperature |
| $T_I$ | = | interfacial temperature |
| $T_{SAT}$ | = | saturation temperature |
| $u$ | = | velocity |
| $X_{v,s}$ | = | interfacial mole fraction |
| $z$ | = | axial position along pipe |
| $\alpha$ | = | void fraction |
| $\delta_F$ | = | liquid film thickness |
| $\Gamma_{cond}$ | = | rate of condensation per unit mixture volume |
| $\rho$ | = | density |
| $\tau$ | = | time(s) |
| $\Delta\tau$ | = | time step(s) |

## I. Introduction

Condensation in the presence of noncondensables is a common phenomenon in nature and industry. Condensers in steam power cycles, for example, operate at low pressures and as a result are vulnerable to the inward leakage of air and the accumulation of air in the condenser flow passages. In large condensers the noncondensables preferentially accumulate in the parts of the condenser where the flow rate is low. Noncondensable-rich pockets can thus form in these parts of the condenser and lead to the air blanketing phenomenon, whereby rendering those condenser segments essentially ineffective. Even without noncondensable blanketing, the presence of noncondensables in the vapor, at a few percent mass fraction, leads to a significant reduction in the efficiency of the condenser. Condensation in the presence of noncondensables is also of particular interest when the recovery of water from steam-noncondensable gas mixtures is intended. Other applications of interest include but are not limited to moisture removal and in-situ propellant recovery for deep space missions.

The presence of small amounts of noncondensables reduces the condensation rate significantly. The flow of vapor towards the cold surface where condensation is to occur results in the accumulation of the noncondensables near the interphase between the gas-vapor mixture and the condensate. This forms a noncondensable-rich gas-vapor film. Consequently, the vapor will need to overcome a mass transfer resistance and diffuse through this noncondensable-rich film before it can condense at the interphase. The presence of noncondensables thus renders the condensation process into a combined heat and mass transfer process. A detailed discussion of condensation in general, and condensation in the presence of noncondensables can be found in Ghiaasiaan[1].

A widely-applied engineering method for modeling condensation in the presence of noncondensables is the Couette flow film model (also referred to as the stagnant flow film model). This technique has been shown to do well when applied to external as well as internal flow condensation processes. The model has also been successfully implemented in computer codes that apply the two-fluid modeling technique for the treatment of flow condensation[2,3]. More recent applications of the stagnant film model include condensation in the containment of nuclear reactors[4].

In this paper we report on the implementation of the Couette flow film model for condensation in the presence of noncondensables in the GFSSP computer code,[7] and its validation against experimental data.

# II. Theory

## A. General Remarks

GFSSP is a general purpose computer program that analyzes transient and steady state flow rates, pressures, temperatures, concentrations, and conjugate heat transfer in complex flow networks. It employs a finite volume formulation of the mixture mass, mixture momentum, and mixture energy conservation equations coupled with thermodynamic equations of state for real fluids. These systems of equations are solved using a hybrid numerical algorithm using a combination of the Newton-Raphson and successive substitution methods. GFSSP contains a graphical user interface that allows the user to "point, drag, and click" various components of the model into place. These components are divided into nodes, branches, and conductors which compute scalar properties, mass flow rates, and heat transfer rates, respectively. Fig. 1 provides a depiction of a typical counter-flow annular heat exchanger model displayed by GFSSP. The program was developed at the NASA Marshal Space Flight Center in 1994 and has been successfully verified through 30 example problems. Its ability to allow the implementation of user subroutines (using FORTRAN) greatly enhances its capacity to model a vast variety of practical and specific applications.

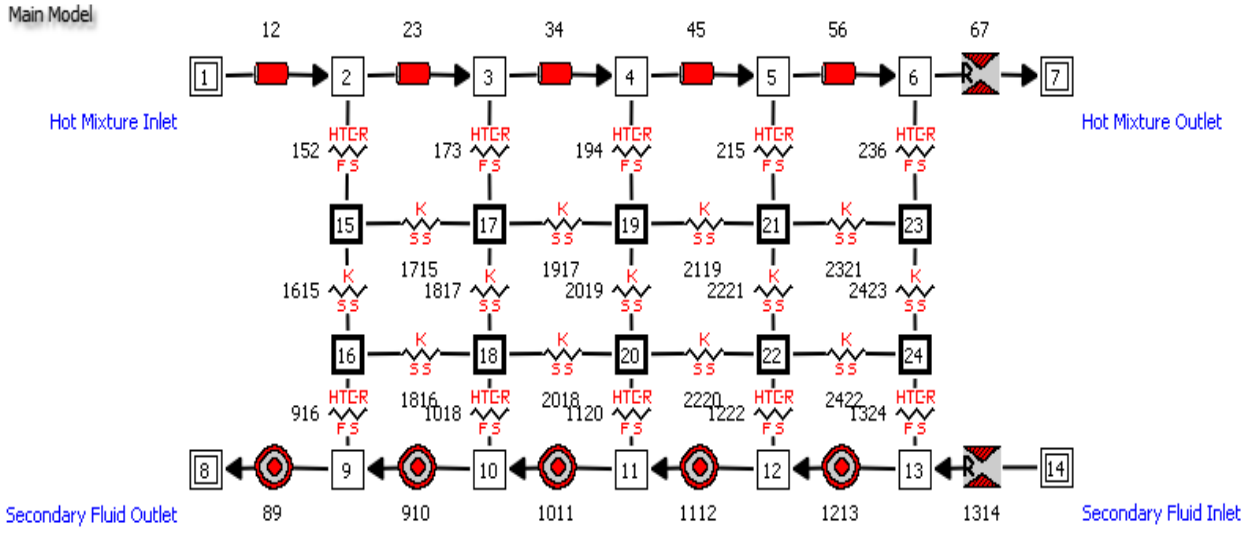


Figure 1: Counter flow heat exchanger model displayed in GFSSP

Currently the condensation model has been implemented as a routine with one-way coupling to GFSSP. When condensation in a flow passage is of interest, for example, the condensation subroutine receives information about the pressure, flow rate, and flow properties at the inlet to the flow passage (i.e., the first node in the flow passage) from GFSSP, as well as the pressure and wall temperature at every node in the condensing flow passage. The wall inner surface temperature distribution can also be provided to the condensation subroutine as a user input. The condensation routine then solves the Couette flow film model equations (discussed below) at every node and every time step, thus calculating the condensation rate in each node. Although GFSSP rigorously keeps track of the mass conservation and concentration of vapor and noncondensables, the program does not currently separate the condensable species into vapor and liquid phases. To circumvent this issue, the condensation subroutine independently solves the mass conservation equations for the condensate, vapor, and the noncondensable, thus keeping track of the buildup of the noncondensable concentration along the condensation flow passage.

## B. Couette Flow Film Model

Only the outline of the model is presented here, and a detailed discussion can be found in (Ref. 1). The implementation of the model follows Refs. (2,3), where the model has been successfully implemented for the treatment of condensing two-phase flows in computer codes that are based on two-fluid modeling.

Fig. 2 depicts a schematic of the temperature and concentration profiles at the vicinity of the condensate-vapor/noncondensable mixture interphase during condensation on a cold surface, where for simplicity and convenience the condensate is depicted as a falling liquid film. Although a liquid film is the predominant flow regime for the condensate in most terrestrial condensation processes, the model to be described is general and can be applied to other flow regimes as well.

It is assumed that the noncondensable has essentially zero solubility in the condensate liquid. As mentioned earlier, a noncondensable-rich film of gas-vapor mixture forms next to the interphase and the vapor molecules need to diffuse through this layer before they can reach the interphase. The accumulation of the noncondensables near the interphase leads to the reduction of vapor pressure at the interphase. Because the interphase must be at saturation conditions with respect to the local vapor pressure, the interphase temperature will be reduced as well. The overall effect of the presence of noncondensables is often a significant reduction in the condensation rate, even when the concentration of the noncondensable in the vapor-noncondensable bulk is very small.

Application of energy and mass conservation to the interphase, and taking into account the effect of mass transfer on the convective heat and mass transfer processes (effect of transpiration), leads to the following set of six coupled equations that need to be solved simultaneously.

$$T_{\mathrm{I}} = T_{\mathrm{sat}}(X_{\mathrm{v,s}}P) \tag{1}$$

$$\dot{h}_{\mathrm{GI}}(\bar{T}_{\mathrm{G}} - T_{\mathrm{I}}) - \dot{h}_{\mathrm{FI}}(T_{\mathrm{I}} - \bar{T}_{\mathrm{F}}) + m^{"}\boldsymbol{h}_{\mathrm{fg}} = 0 \tag{2}$$

$$m^{"} = -K_{\mathrm{GI}} \ln \frac{1 - m_{\mathrm{v,G}}}{1 - m_{\mathrm{v,s}}} \tag{3}$$

$$m_{\mathrm{v,s}} = \frac{X_{\mathrm{v,s}}M_{\mathrm{v}}}{X_{\mathrm{v,s}}M_{\mathrm{v}} + (1 - X_{\mathrm{v,s}})M_{\mathrm{n}}} \tag{4}$$

$$\dot{h}_{\mathrm{GI}} = \frac{-m^{"}C_{Pv}}{\exp\left(\frac{-m^{"}C_{Pv}}{h_{\mathrm{GI}}}\right) - 1} \tag{5}$$

$$\dot{h}_{\mathrm{FI}} = \frac{m^{"}C_{P\mathrm{F}}}{\exp\left(\frac{m^{"}C_{P\mathrm{F}}}{h_{\mathrm{FI}}}\right) - 1} \tag{6}$$

In these equations $h_{\mathrm{GI}}$ and $h_{\mathrm{FI}}$ represent the interphase-mixture and interphase-film convective heat transfer coefficients, respectively, at the limit of vanishing mass transfer (i.e., vanishing condensation rate). The quantities $\dot{h}_{\mathrm{GI}}$ and $\dot{h}_{\mathrm{FI}}$ are defined similarly, but they account for the effect of mass transfer. The parameter $K_{\mathrm{GI}}$ represents the vapor mass transfer coefficient between gas-vapor bulk and the interphase, also at the limit of negligible mass transfer rate through the interphase. The unknowns in Eqs. (1 – 6) are $T_{\mathrm{I}}, m_{\mathrm{v,s}}, X_{\mathrm{v,s}}, m^{"}, \dot{h}_{\mathrm{GI}}$, and $\dot{h}_{\mathrm{FI}}$.

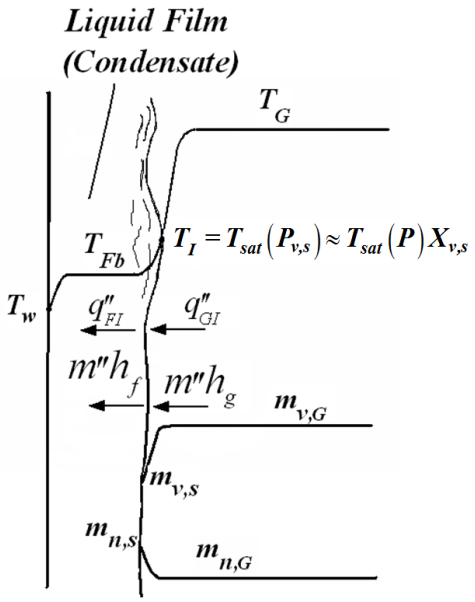


Fig. 2. Schematic of the temperature and species concentration profiles during condensation in the presence of a noncondensable.

### C. Implementation in GFSSP

The following is GFSSP's formulation of the mass, momentum, and energy equations tailored to the model of condensation, respectively. The accompanying Fig. 3 displays a schematic showing adjacent nodes, connecting branches, and the indexing system:

$$\frac{m_{\tau+\Delta\tau} - m_\tau}{\Delta\tau} = -\sum_{j=1}^{j=N} \dot{m}_{ij} \tag{7}$$

$$\frac{(mu)_{\tau+\Delta\tau} - (mu)_\tau}{\Delta\tau} + MAX|\dot{m}_{ij}, 0|(u_{ij} - u_u) - MAX|-\dot{m}_{ij}, 0|(u_{ij} - u_u) = (P_i - P_j)A_{ij} - K_f \dot{m}_{ij}|\dot{m}_{ij}|A_{ij} \tag{8}$$

$$\frac{\left(m_i h_{ik} - \frac{P}{\rho_k J}\right)_{\tau+\Delta\tau} - \left(m_i h_{ik} - \frac{P}{\rho_k J}\right)_\tau}{\Delta\tau} = \sum_{j=1}^{j=N} MAX|-\dot{m}_{ij}, 0|h_{jk} - MAX|\dot{m}_{ij}, 0|h_{ik} \tag{9}$$

The mass and momentum equations are simultaneously solved to calculate system respective pressures and mass flow rates. Next, the energy equation is solved for each species to compute enthalpies, and mixture temperatures can be extracted thereafter. GFSSP's conjugate heat transfer capabilities can then solve for the inner wall temperatures needed for the condensation subroutine. Inner wall temperatures can also be specified by the user in a separate subroutine if desired. As discussed earlier, GFSSP cannot differentiate between the phases of the condensable as far as mass fraction is concerned, so mixture mass fraction is tracked within the condensation subroutine. Since the vapor in the free stream is always assumed to be saturated, the free stream nodal temperatures can be determined with nodal pressures provided by GFSSP. The mixture mass flow rates in each branch are also read from GFSSP by the condensation subroutine. Knowledge of the nodal total pressures, mixture mass flow rates, and inner wall temperatures are sufficient to solve Equations (1-6).

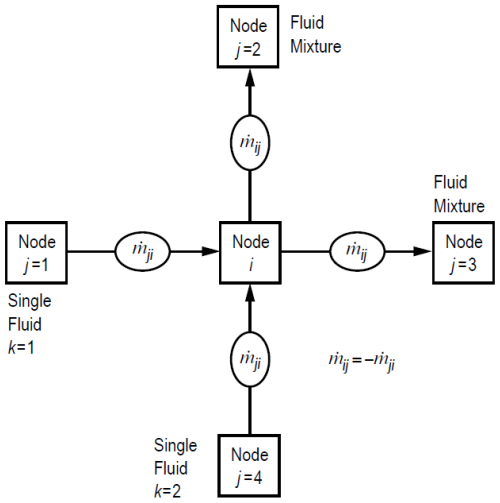


Figure 3: Indexing system for the mathematical formulation in GFSSP

The solving of Equations (1-6) thus lead to the calculation of the condensation mass flux at the condensate-vapor-noncondensable interphase. The condensation rate per unit mixture volume is then found from

$$\Gamma_{cond} = a_I'' m'' \tag{10}$$

where $a_I''$ represents interfacial area concentration (i.e., the interfacial area per unit two-phase mixture volume), which is flow regime dependent. As a result, in general, a flow regime map is needed for the calculation of the condensation flows. For an ideal annular flow in a circular pipe, assuming axisymmetric flow, we have

$$a_I'' = \frac{\sqrt{\alpha}}{D} \tag{11}$$

where α is the void fraction, and $D$ is the tube inner diameter. The void fraction is related to the liquid film thickness according to

$$\alpha = 1 - \left(\delta_F / D\right)^2 \tag{12}$$

For a steady-state condensing flow in an axisymmetric circular pipe the following equations are solved independently by the condensation routine.

$$\frac{d}{dz}\dot{m}_L = A a_I'' m'' \tag{13}$$

$$\frac{d}{dz}\dot{m}_G m_{v,G} = -A a_I'' m'' \tag{14}$$

$$\dot{m}_G m_{n,G} = const. \tag{15}$$

Furthermore, as previously stated, the gas-vapor mixture is assumed to remain saturated, therefore

$$T_G = T_{sat}(x_{v,G}P) \tag{16}$$

Equations (1-6) are solved iteratively in every time step, and for every node where condensation is underway. These equations are solved using the method of repeated bisections. Equations (13-15) are discretized using the finite-volume technique, consistent with the solution method in GFSSP.

The general solution method for the method of repeated bisections is as follows. It is known that the mixture-film interface temperature (one of the six unknowns) must be bounded between the inner wall and mixture temperatures. Thus the condensation subroutine is first run twice, with an interface temperature guess as the wall temperature and the mixture temperature. Since the interface temperature is being provided, Equations (1-6) can be solved directly, and Equation (2) was chosen to act as a residual equation. A correct guess of the interface temperature would result in a zero residual, i.e., the left-hand and right-hand sides of Equation (2) would be equal. Our two initial guesses for the interface temperature are knowingly wrong but guarantee exactly one positive and one negative residual, ensuring a bounded solution. The condensation subroutine is then run a third time, and the interface temperature guess is now at the bisected temperature of the first two guesses. Based on the sign of the residual for this guess, it can be determine whether the guess was too high or too low. The just-guessed interface temperature then becomes either the new upper bound or new lower bound, respectively. The condensation subroutine is then run again at the new bisected temperature, and this process is repeated until the zero residual is found, to the desired accuracy.

## III. Model Validation

### A. Experimental Data

Experimental data of Siddique[7] and Ogg[8] are used for model validation. The experimental data and the selected test runs are similar to those used in Refs. (2,3) for the validation of the Couette flow film model that had been incorporated in a two-fluid model for condensing two-phase flow. Important test section geometric characteristics of the experimental test rigs are summarized in Table 1. The test sections in these experiments were circular, vertical metallic tubes that had annular jackets. The condensing two-phase mixture flowed downward inside the circular tubes, while the tubes were cooled by a countercurrent flow of a liquid coolant that flowed in their annular jackets. The wall inner surface temperatures were measured at several points along the test sections. The reported wall inner surface temperatures for the tests of Siddique[7] and Ogg[8] are used as the flow passage boundary condition here.

| Test characteristic | Siddique[5] | Ogg[6] |
|---|---|---|
| Test section tube material | SS 304 | SS 321 |
| Total tube length [m] | 2.54 | 5.2 |
| Length of cooled segment of tube [m] | 2.44 | 2.44 |
| Inner diameter [m] | 0.046 | 0.049 |
| Wall thickness [m] | 0.0024 | 0.00071 |
| Temperature measurement location from test section entrance [cm] | 10.0 and then at each 30.5 cm step | 0.0 and then at each 5 cm step |

Table 1. Important experimental test section geometric parameters

| Source | Test no. | Pressure [kPa] | Mixture flow rate [kg $s^{-1}$] | Noncondensable mass fraction |
|---|---|---|---|---|
| Siddique[5] | 6 | 133 | 0.00378 | 0.332 |
| | 26 | 233 | 0.00740 | 0.224 |
| | 41 | 213 | 0.00937 | 0.099 |
| Ogg[6] | 12-4 | 108 | 0.0131 | 0.179 |
| | 17-1 | 252 | 0.0203 | 0.017 |
| | 19-4 | 139 | 0.0111 | 0.018 |

Table 2. The test section inlet conditions for the experiments used for model validation.

## B. Simulations

Fig. 4 depicts the GFSSP representation of the flow channels in the experiments. The GFSSP model divides the flow channel into 25 nodes, with 26 branches that connect the adjacent nodes. GFSSP is capable of solving conjugate heat transfer problems, and the model depicted in Fig. 4 represents both the primary (condensing flow pipe) and secondary (the annulus) flows. The condensation model, however, runs parallel to GFSSP and currently is one-way coupled to GFSSP.

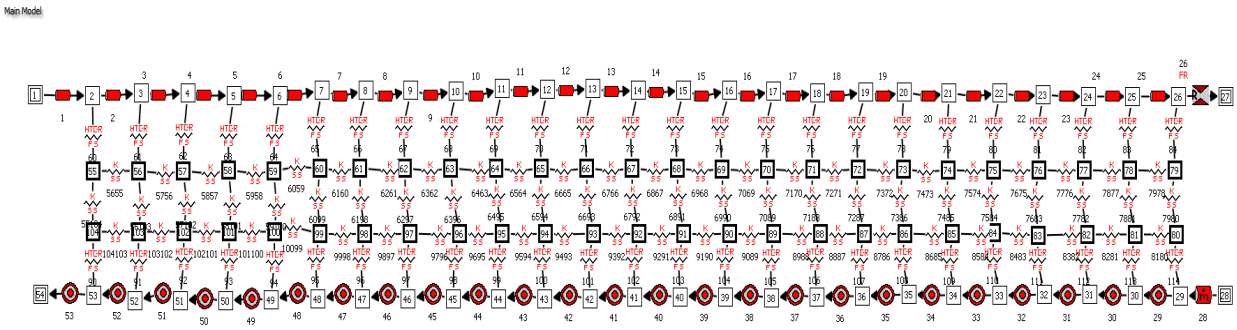


Figure 4. GFSSP model used to solve the Couette flow model condensation equations

## C. Results and Discussion

Figs. 5 and 6 below show the GFSSP model results for an air-vapor mixture against the experimental data of Siddique and Ogg, respectively.

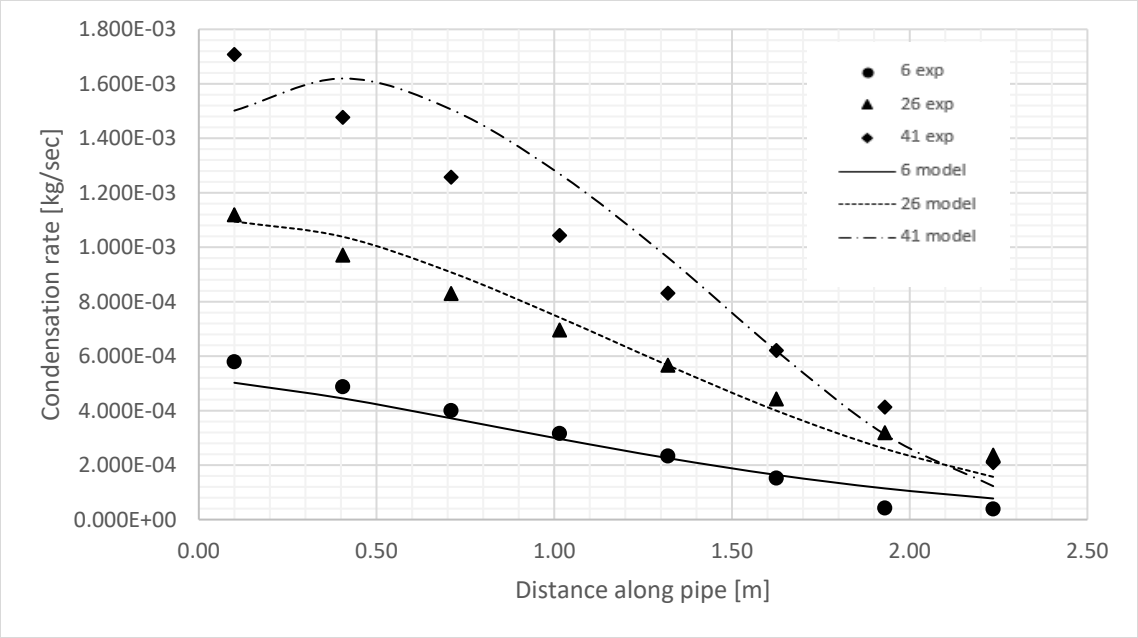


Figure 5. Air-steam mixture concentration rate vs. distance from Siddique

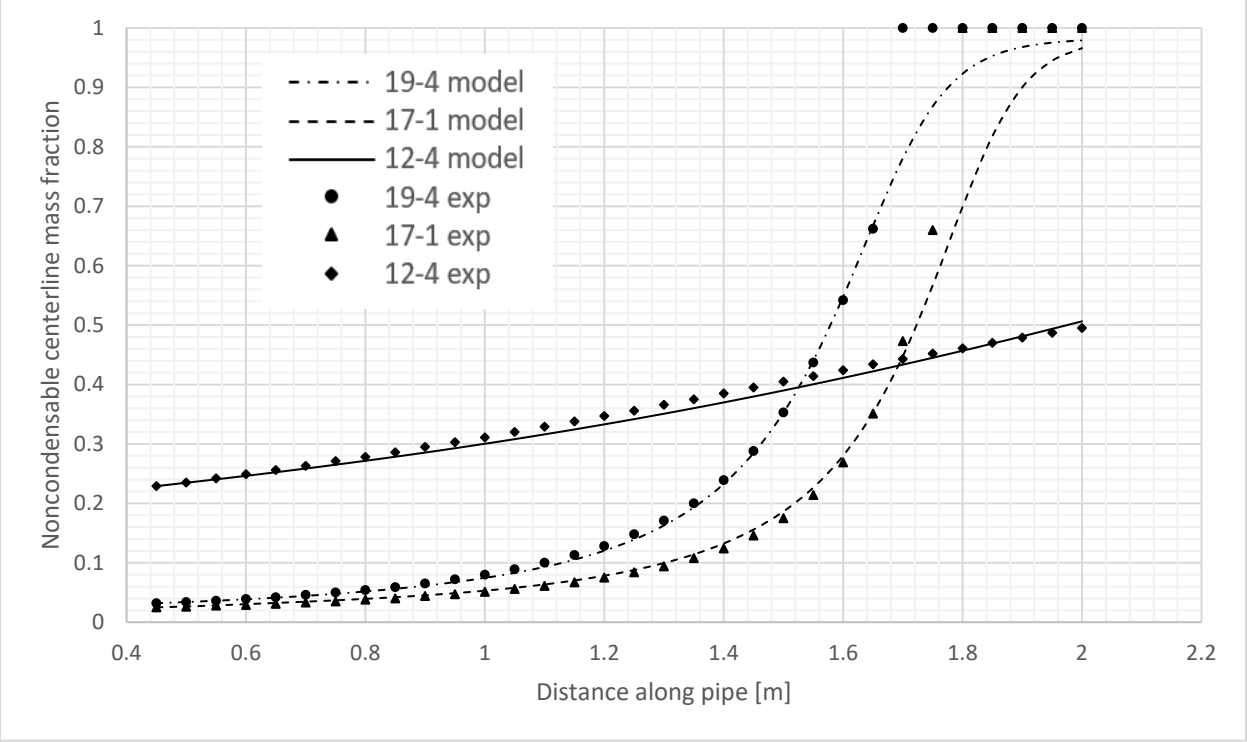


Figure 6. Air-steam mixture noncondensable mass fractions vs. distance from Ogg

As seen, the GFSSP model agrees quite well with experimental data. The model appears to deviate from Ogg's data when the condensation rate is sufficiently large. In these instances, Ogg's experiments show sudden, full condensation where the GFSSP model predicts an asymptotic approach towards full condensation. In the one case

presented here where the vapor did not fully condense, the agreement is very good. The model agreement with Siddique's experiment is also good, with the most deviation in the case of a higher mass flow rate and lower initial mass fraction of noncondensable. However, the cases displayed here by Ogg contain even higher flowrates and lower noncondensable mass fractions and show excellent agreement. This suggests possible experimental error and a lack of experimental information needed for the condensation model to produce an accurate solution. The wall temperature readings provided from Siddique were spread far enough apart such that either a coarse GFSSP model was required or linear interpolation of the inner wall temperatures from the data provided was required. The coarse model assumes relatively large (0.3 m) segments of pipe contain constant thermal properties, which undoubtedly could lead to inaccurate data. However any model finer than 0.3 m would require a guess of inner wall temperatures, which also leads to discrepancy. When compared to Ogg's data, where much more experimental data was provided, it can be seen that the model has much better agreement.

## IV. Conclusions

A model for condensation in the presence of noncondensables, based on the Couette flow film (stagnant film) model, has been developed and coded for the Generalized Fluid System Simulation Program (GFSSP) computer code. The developed computer routine is consistent with GFSSP and can be coupled to that code. The coupling with GFSSP is one way, whereby the condensation modle receives information from GFSSP including the nodal pressure, temperature and mass concentrations, and calculates the condensation rate in each node. The model was validated against experimental data representing steady-state condensation of water vapor in downward flow of air-water vapor and mixtures in vertical tubes, with good agreement between data and model predictions.

## V. References


1. Ghiaasiaan, S.M. *Two-Phase Flow, Boiling and Condensation in Conventional and Miniature Systems.* 2nd ed. Cambridge University Press, Cambridge, United Kingdom, 2017.
2. Ghiaasiaan, S. M., Kamboj, B. K. and Abdel-Khalik, S. I., "Two-Fluid Modeling of Condensation in the Presence of Noncondensables in Two-Phase Channel Flows," Nuclear Science and Engineering, Vol. 119, 1995, pp. 1-17.
3. Yao, G.F., Ghiaasiaan, S.M. and Eghbali, D.A., "Semi-Implicit Modeling of Condensation in the Presence of Noncondensables in the RELAP5/MOD3 Computer Code," Nuclear Engineering and Design, Vol. 166, 1996, pp. 277-291.
4. Lee, J., Park, G.-C., and Cho, H.K., "Implementation of CUPID code for Simulating Filmwise Steam Condensation in the Presence of Noncondensable Gases," Nuclear Engineering Technology, Vol. 47, 2015, pp. 567-578.
5. Siddique, M., "The Effects of Noncondensable Gases on Steam Condensation under Forced Convection Conditions," PhD Thesis, Massachusetts Institute of Technology, Department of Nuclear Engineering, Cambridge, Massachusetts, 1992.
6. Ogg, D.G., "Vertical Downflow Condensation Heat Transfer in Gas-Steam Mixtures," MS Thesis, University of California, Department of Nuclear Engineering, Berkeley, CA, 1991.
7. Generalized Fluid System Simulation Program, Version 6.0, A.K. Majumdar, A.C. LeClair, and R. Moore. Marshall Space Flight Center, Huntsville, Alabama.